An improved weighting coefficient optimization-particle filtering algorithm based on Gaussian degradation model for remaining useful life prediction of lithium-ion batteries.

GAO, H., WANG, S., QIAO, J., YANG, X. and FERNANDEZ, C.

2022

An Improved Weighting Coefficient Optimization-Particle Filtering Algorithm Based on Gaussian Degradation Model for Remaining Useful Life Prediction of Lithium-ion Batteries

Journal:	*Journal of The Electrochemical Society*
Manuscript ID	JES-108996.R1
Manuscript Type:	Research Paper
Date Submitted by the Author:	08-Nov-2022
Complete List of Authors:	Gao, Haiying; Southwest University of Science and Technology, Wang, Shunli; Southwest University of Science and Technology Qiao, Jialu; Southwest University of Science and Technology Yang, Xiao; Southwest University of Science and Technology Fernandez, Carlos; Robert Gordon University
Keywords:	lithium-ion battery, remaining useful life, improved weighting coefficient optimization algorithm, particle filtering, Gaussian degradation model

An Improved Weighting Coefficient Optimization-Particle Filtering Algorithm Based on Gaussian Degradation Model for Remaining Useful Life Prediction of Lithium-ion Batteries

Haiying Gao,[1] Shunli Wang,[1,2,z] Jialu Qiao,[1] Xiao Yang, [1] and Carlos Fernandez[3]

[1]School of Information Engineering, Southwest University of Science and Technology, Mianyang 621010, China
[2]College of Electrical Engineering, Sichuan University, Chengdu 610065, China
[3]School of Pharmacy and Life Science, Robert Gordon University, Aberdeen AB10-7GJ, United Kingdom

[z]E-mail: 497420789@qq.com

Abstract: Establishing a capacity degradation model accurately and predicting the remaining useful life of lithium-ion batteries scientifically are of great significance for ensuring safety and reliability throughout the batteries' whole life cycle. Aiming at the problems of "particle degradation" and "sample poverty" in traditional particle filtering, an improved weighting coefficient optimization - particle filtering algorithm based on a new Gaussian degradation model for the remaining useful life prediction is proposed in this research. The main idea of the algorithm is to weight the selected particles, sort them according to the particle weights, and then select the particles with relatively large weights to estimate the filtering density, thereby improving the filtering accuracy and enhancing the tracking ability. The experimental verification results under the National Aeronautics and Space Administration data show that the improved weighting coefficient optimization - particle filtering algorithm based on the Gaussian degradation model has significantly improved accuracy in predicting the remaining useful life of lithium-ion batteries. The RMSE of the B05 battery can be controlled within 1.40% and 1.17% at the prediction starting point of 40 cycles and 70 cycles respectively, and the RMSE of the B06 battery can be controlled within 2.45% and 1.93% at the prediction starting point of 40 cycles and 70 cycles respectively. It can be seen that the algorithm proposed in this study has strong traceability and convergence ability, which is important for the development of high-reliability battery management systems.

1 Introduction

With the increasingly serious environmental pollution and the greenhouse effect, the vigorous development of new energy has become an irreversible trend of the times[1-3]. As one of the tracks of the "dual carbon" goal, new energy vehicles have ushered in new opportunities and challenges[4]. The lithium-ion battery is one of the "three electricity" core components of new energy vehicles[5, 6]. Compared with traditional fuel cells, lithium-ion batteries have the advantages of large energy density, low self-discharge

rate, long life cycle, energy conservation and environmental protection[7, 8]. It is the electrochemical energy storage component with the fastest development in recent years[9, 10]. However, with the progress of cyclic charging and discharging, the battery will be aging inevitably, and the safety performance will be greatly reduced, especially the useful life will be significantly shortened when working at low temperatures [11]. The inaccurate prediction of remaining useful life (RUL) may cause the batteries to work in the environment below the capacity failure threshold, which leads to batteries ignition or even explosion[12, 13]. Therefore, accurate prediction of the RUL of lithium-ion batteries is the basis for the safety, operation and maintenance of the battery management system (BMS).

The RUL of lithium-ion batteries refers to the number of charging and discharging cycles that occur before the health of the batteries deteriorates to a point where the device cannot continue to work or the failure threshold is not met[14, 15]. At present, the research methods of the RUL by domestic and foreign scholars mainly include model-based methods, data-driven methods and fusion prediction methods. The data-driven method doesn't need to focus on the aging mechanism inside the batteries, but only depends on the batteries' history degradation data to build the aging prediction model[16, 17]. There are many data-driven methods, including artificial neural networks, autoregression models, support vector machines, Gaussian regression models and so on[18, 19]. However, these methods often use complex signal processing techniques to extract features from sensor data, which requires a large amount of time and highly depends on the accuracy of the data. Fusion-based methods mainly make up for the shortcomings of single-model prediction and the limitations of single data-driven prediction by effectively fusing multiple prediction methods[20]. They can improve the accuracy and generalization ability of prediction, but at the same time, the complexity of the algorithm and the sources of error will increase dramatically[21].

The model-based method is widely used in the RUL prediction of lithium-ion batteries due to its low computational complexity and high prediction accuracy. It describes the degradation process of batteries by establishing a mathematical model of the degradation process, which can be divided into three categories: electrochemical model, equivalent circuit model, and empirical degradation model[22-24]. The electrochemical model establishes a degradation model by analyzing the electrochemical properties of lithium-ion batteries, which can give a detailed physical and chemical analysis of the battery aging process[25]. However, the relevant models are based on specific battery materials, operating environments, and charging-discharging conditions, which make it difficult to obtain model parameters and poor dynamic certainty[26]. The equivalent circuit model is composed of electrical components built based on the system working principle through the analysis of a large amount of state data by experts with specialized

knowledge, which is highly achievable, but some internal or external influencing conditions of the battery may be ignored in the approximation process, resulting in the weak descriptive ability of the model for the dynamic and static characteristics of the batteries[27, 28]. The empirical degradation model achieves the model representation of battery degradation characteristics by describing the change law of state variables that represent the degradation of battery performance with time or by describing the relationship between state variables before and after two moments. This type of model is easy to obtain and has a wide range of applications, which seeks the regularity of data collection over time or the recursive relationship of the internal state of the system[29, 30].

In [31], a model-based method is used to establish mathematical and physical models to describe the degradation process of lithium-ion batteries. Data-driven methods are used to extract useful information such as the order of the model, and the relationship between current and voltage components, and update the model parameters by measuring data. The RUL of lithium-ion batteries is reflected by health indicators, available capacity and internal endurance capacity. In [32], a novel RUL prediction model is proposed by combining the extraction of health indicators based on incremental capacity curve (IC) and the method of improved adaptive relevance vector machine (RVM), which extracts four groups of health indicators based on IC curves that extract from experimental data, and uses Pearson correlation analysis to determine the strong correlation between health indicators and capacity degradation. Then the RVM regression model with Bayesian algorithm is established to optimize kernel parameters. In [33], a new RUL prediction model is formed by combining the particle filter and neural network based on the filter algorithm, using particle filtering to provide a real-time framework and neural network to establish an appropriate parameter measurement equation. In [34], an improved prediction method combining linear optimized resampling particle filter (LORPF) and sliding window grey model (SGM) was proposed. The measurement function of LORPF is derived using the SGM development factor, and the state transition function of LORPF is established using the exponential growth model to track capacity degradation. The SGM-LORPF framework uses only a small amount of historical data to obtain accurate results.

To realize high accuracy estimation of the RUL of lithium-ion batteries, the capacity degradation model and the remaining service life prediction algorithm are studied in this study, and the following two points are proposed: (1) A new Gaussian degradation model is proposed, which has a better description of the non-linear degradation characteristics of lithium-ion batteries capacity than the double exponential degradation model. (2) An improved weighting coefficient optimization - particle filter algorithm (WCO-PF) is proposed, which overcomes the problems of "particle degradation" and "sample poverty" of

traditional particle filtering, and ensures the estimation accuracy of the RUL of lithium-ion batteries. Finally, experimental verification was carried out with the data set provided by the National Aeronautics and Space Administration (NASA).

The paper is organized as follows, Section 2 is the theoretical analysis, including the Gaussian degradation model and improved WCO-PF algorithm. Section 3 is the experimental results and analysis. Section 4 is the conclusion.

2 Theoretical analysis

2.1 Gaussian degradation modeling

The lithium-ion batteries have strong nonlinear characteristics, and the use of nonlinear models can more accurately characterize their dynamic behavior for nonlinear systems. The commonly used lithium-ion battery degradation model is the double exponential degradation model[35], and its model structure is shown in Equation (1).

$$Q_k = ae^{bk} + ce^{dk} \tag{1}$$

In Equation (1), k represents the number of charging and discharging cycles, Q_k is the battery capacity at k cycles, a、b、c、d indicates unknown parameters. Although the double exponential degradation model has been widely used, the system robustness is poor, and small changes in model parameters can cause large fluctuations in the prediction results[36]. In order to accurately estimate the RUL of lithium-ion batteries, it is very important to establish an accurate capacity attenuation model. Through the analysis of experimental data and the testing of various models, the Gaussian degradation model shown in Equation (2) is proposed to characterize the capacity degradation process of lithium-ion batteries.

$$Q_k = a_1 e^{-\left(\frac{k-b_1}{c_1}\right)^2} + a_2 e^{-\left(\frac{k-b_2}{c_2}\right)^2} \tag{2}$$

In Equation (2), k represents the number of charging and discharging cycles, Q_k is the battery capacity at k cycles, a_1, b_1, c_1, a_2, b_2, c_2 indicates unknown parameters. Compared with the traditional double exponential degradation model, this model is more stable and robust, and it will not cause the over-fitting problem of the model due to many parameters, which are easy to the identification of the model parameters[37].

2.2 An Improved Weighting Coefficient Optimization - Particle Filtering Algorithm

Particle filtering has become a mainstream algorithm for solving the optimal estimation problem of the nonlinear non-Gaussian state space model. However, the traditional particle filtering algorithm has the

defects of "particle degradation" and "sample poverty", resulting in low accuracy of RUL prediction of lithium-ion batteries. To achieve the high precision prediction of RUL, an improved WCO-PF algorithm is proposed to improve the filtering accuracy and enhance the tracking ability. The main idea of the algorithm is to optimize the weight coefficients of the selected particles, weight the selected N_s particles according to Sequential Importance Sampling (SIS), sort the particle weights, and then select the first N_p ($N_p < N_s$) particles with larger weights to estimate the filter density while allowing all candidate particles to participate in the particle update process at the next moment. The flow chart of the algorithm is shown in Figure 1.

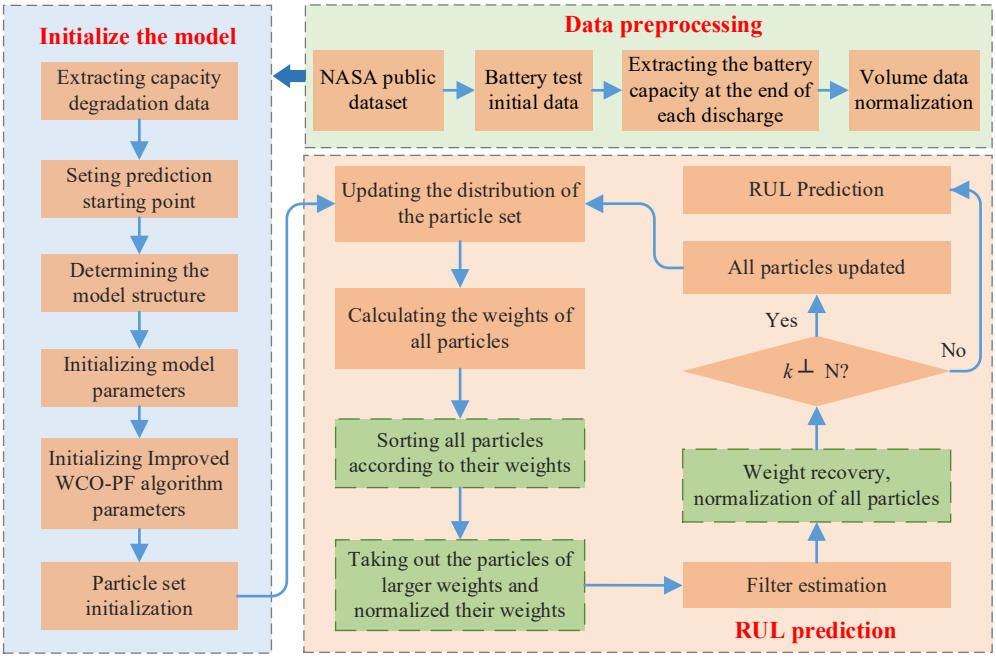

Figure 1. The flow chart of the improved WCO-PF algorithm

In Figure 1, k represents the number of cycles of the algorithm and N represents the total number of cycles of the battery experiment. As shown in Figure 1, the Gaussian degradation model is combined with the improved WCO-PF algorithm to estimate the RUL of lithium-ion batteries. The prediction method mainly includes data preprocessing, initialization model and RUL estimation. The parameters of the capacity degradation model are updated as the state vector, and the capacity data before the prediction starting point (SP) T is used as the model training data. System initialization is shown in Equation (3).

$$\begin{cases} x_0 = [a_{1,0}, b_{1,0}, c_{1,0}, a_{2,0}, b_{2,0,}, c_{2,0}]^T \\ w_0 = 1/N_s \end{cases} \tag{3}$$

In Equation (3), x_0 is the initialization state vector, and the initial value is the parameter identification results. Selecting N_s particles as the particle set, and the initial weight of all particles is $1/N_s$. After the system is initialized, the distribution of the particle set at this time is updated according to the importance of probability density with reference to the particle state at the previous time. The system state equation is

shown in Equation (4).

$$x_k^i = \mathrm{f}\left(x_{k-1}^i, u_{k-1}\right) + o_{k-1} \tag{4}$$

In Equation (4), x_k^i is the state of $\mathrm{N_s}$ particles at time k, where the interference during battery operation is described by Gaussian noise with zero mean. According to the SIS process, the weights of $\mathrm{N_s}$ particles at time k are calculated by the recursive update method, as shown in Equation (5).

$$\begin{cases} err_k^i = y_k - \hat{y}_k^i = y_k - \mathrm{h}\left(\hat{x}_k^i\right) \\ w_k^i = w_{k-1}^i \dfrac{\mathrm{p}\left(y_k|x_k^i\right)\mathrm{p}\left(x_k^i|x_{k-1}^i\right)}{\mathrm{q}\left(x_k^i|x_k^{i-1}, y_k\right)} \end{cases} \tag{5}$$

In Equation (5), w_k^i is the weight coefficient of the particles, y_k is the actual RUL value of the batteries, $\hat{y}_k^i$ is the observed value of the system. However, with the increase of the number of iterations, the variance of the particle importance weight will gradually increase, resulting in particles with larger weights at the beginning getting larger and larger weights during the iteration process, and only a few particles have large weights, while lots of computing resources are wasted on particles with almost zero weights. This is the serious defect of "particle degradation" of the SIS method. The traditional PF algorithm adopts resampling after SIS to overcome the particle degradation problem, and the process of particle resampling in the PF algorithm is shown in Figure 2.

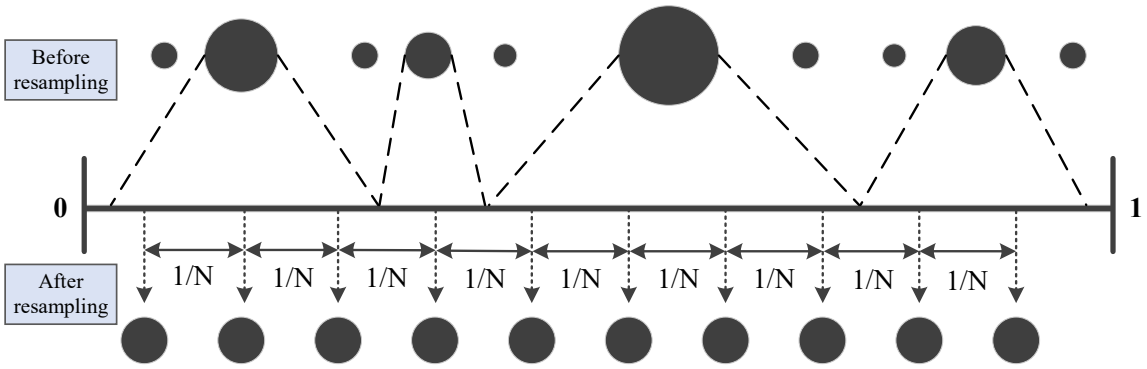

Figure 2. Process diagram of particle resampling in the PF algorithm

As shown in Figure 2, the resampling means that the particles with larger weights are copied proportionally and the particles with smaller weights are discarded, so that the total number of particles remains the same and the particles have reasonable weights. However, the resampling algorithm brings about the problem of "sample poverty", that is, the subset of the particles with high weight is increasing, and the particles with low weight are gradually abandoned, which leads to the poor diversity of the particle set.

The improved WCO-PF proposed in this study solves the two problems of "particle degradation" and "sample poverty". The process of Weighting coefficient optimization process in the improved WCO-PF algorithm is shown in Figure 3.

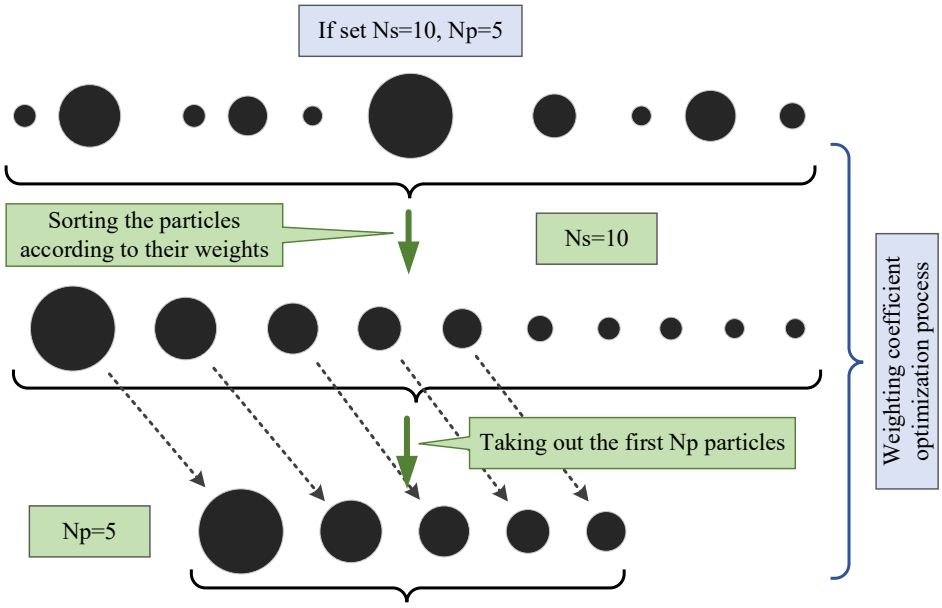

Figure 3. Process diagram of Weighting coefficient optimization process in the improved WCO-PF algorithm

It can be seen from Figure 3, assuming that the number of particles required for a certain estimation is N_p, the N_s particles obtained by sampling according to the weights after SIS is completed are sorted and selects N_p particles with larger weights as the particle set for the estimation. After filtering particles are selected, the weights of N_p particles are normalized according to Equation (6).

$$w_k^i = \frac{w_k^i}{\sum_{m=1}^{N_p} w_k^m} \tag{6}$$

In Equation (6), w_k^i represents the weight of the particle at time k. The algorithm selects particles with relatively large weight coefficients from many alternative particles for state estimation, and the subset of selected particles is fixed in number to solve the particle degradation problem, while each sample is independent of each other to improve the diversity of the sample set. After normalizing the weights, the Monte Carlo method is used to estimate the posterior probability directly, as shown in Equation (7).

$$p(x_k|y_{1:k}) \approx \sum_{m=1}^{N_p} w_k^m \delta(x_k - \tilde{x}_k^m) \tag{7}$$

In Equation (7), $\tilde{x}_k^m$ is the filter particle set at time k, and $\delta(x)$ Dirac function, which means that x is 1 if it meets the conditions, and 0 otherwise. Applied to the RUL estimation, it is the expected value of the current state of N_p particles, so the filtering results can be obtained as shown in Equation (8).

$$x_k^i = \sum_{m=1}^{N_p} w_k^m \tilde{x}_k^m \tag{8}$$

In Equation (8), x_k^i represents the state of particles at time k. After filtering, restore the weights of N_p

particles to those before normalization, and then perform weight normalization for N_s particles, as shown in Equation (9). In the next step of prediction, return to Equation (5) for iteration.

$$\begin{cases} w_k^i = w_k^i \sum_{m=1}^{N_p} w_k^m \\ w_k^i = \frac{w_k^i}{\sum_{m=1}^{N_s} w_k^m} \end{cases} \tag{9}$$

The capacity data before SP=T is used as model training data to adjust model parameters to obtain optimal solutions, and the data after T is used to predict future RUL trends. When predicting the future RUL, simply selecting the filtering results at time T-1 as the estimation value will lead to the limitation of the results. This algorithm makes the overall processing of the data matrix of the previous training results and takes the mean value of the 10 training results before time T to participate in the RUL estimation after time T, to achieve the optimal estimation effect.

In the improved WCO-PF algorithm, all particles participate in the particle update at any time, and each particle in the particle set is independent of each others, which improves the diversity of particles. By optimizing the coefficients of all the particles in the particle set, a subset of the fixed number of particles with larger weights is obtained for filter estimation and state tracking, which ensures the optimal weights of the subset of particles and largely alleviates the particle degradation problem.

3 Experimental results and analysis

3.1 Model fitting effect verification

The lithium-ion battery aging data set used in this study was obtained from NASA. The experiment uses commercially available 18650 lithium-ion batteries with a rated capacity of 2 Ah and conducts cycle life experiments on 4 groups of batteries at a room temperature of 24°C. The battery experimental steps are shown in (1) - (3).

(1) Charging test: the battery is charged at a constant current mode of 1.5 A until the voltage reaches 4.2 V, and then charged at a constant voltage mode until the current drops to 20 mA.

(2) Discharge test: the battery is discharged in a constant current mode of 2 A, and the discharge cut-off voltages of B05, B06, B07 and B18 batteries are 2.7, 2.5, 2.2 and 2.5V respectively.

(3) Impedance measurement: impedance measurement was carried out by electrochemical impedance spectroscopy, and the scanning frequency was 0.1 HZ to 5 kHz.

Repeating the above steps until the battery capacity decreases to about 70% of the rated capacity. The capacity failure threshold of the battery is set to 1.38 Ah. The capacity degradation curves of four groups

of lithium-ion batteries are shown in Figure 4.

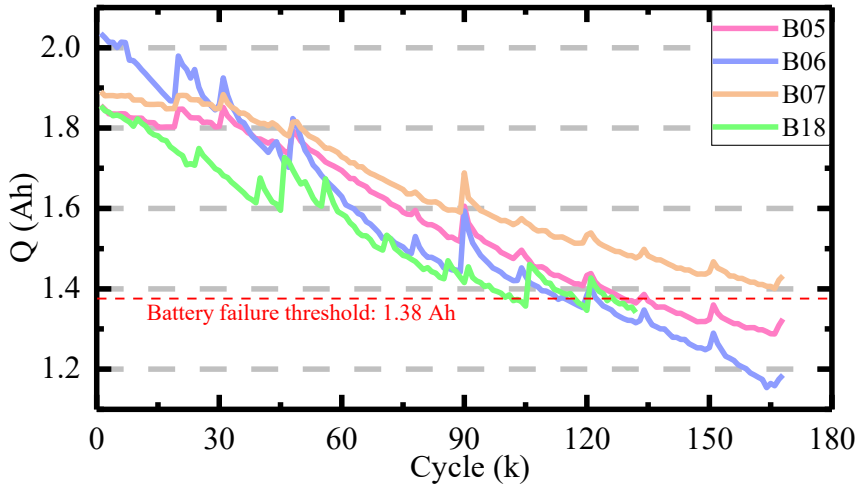

Figure 4. Battery capacity degradation curve

In Figure 4, k represents the number of cycles of the battery experiment, and Q represents the remaining capacity of the battery after each cycle. It can be seen from Figure 4 that the battery threshold is set to 1.38 Ah, and the B07 battery does not meet the analysis conditions. The experimental data of B05 and B06 batteries are selected for subsequent analysis. According to the battery capacity degradation model established in Equation (2), the overall fitting of the battery capacity degradation curve is carried out, and the fitting results of the parameters are shown in Table 1.

Table 1. The parameter fitting results of the Gaussian degradation model

Battery Number	a_1	b_1	c_1	a_2	b_2	c_2
B05	0.123	40.970	37.540	66.930	-3645	1917
B06	1.800	-17.180	92.160	1.200	137.700	111.600

To verify the fitting effect of the proposed model, the battery capacity degradation curves are fitted with the proposed model and the traditional commonly used double exponential degradation model as shown in Equation (1) respectively. The overall fitting effect is shown in Figure 5.

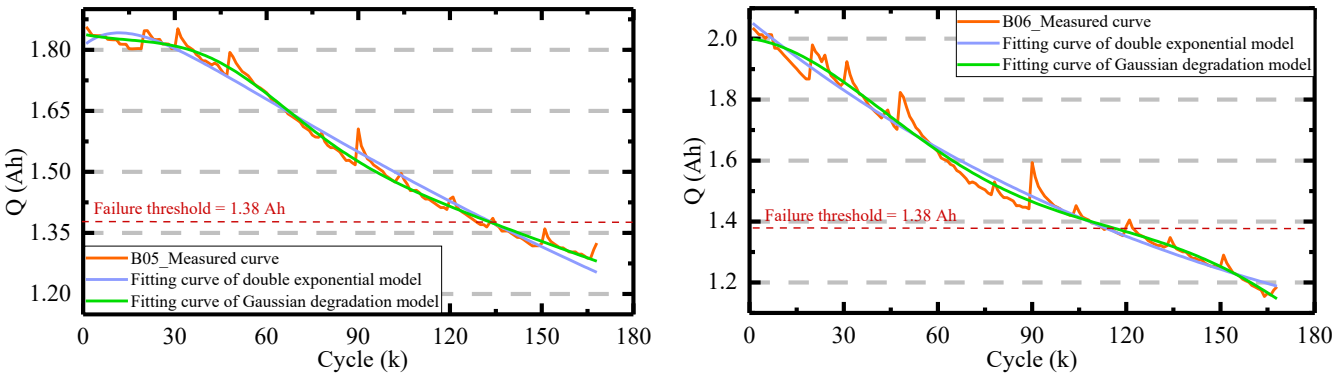

(a) Fitting results of B05 battery (b) Fitting results of B06 battery

Figure 5. Overall fitting effect of battery capacity degradation curve

To compare the fitting results more accurately, the sum of squares due to error (SSE), the R-square (R^2), the adjusted R-square (R^2_{adj}), and the root mean square error (RMSE) are selected as the fitting evaluation indexes. The overall fitting error is shown in Table 2.

Table 2 Overall fitting error of battery capacity degradation curve

Fitting evaluation index	SSE		R^2		R^2_{adj}		RMSE	
Battery number	B05	B06	B05	B06	B05	B06	B05	B06
New capacity degradation	0.03754	0.1456	0.9938	0.9863	0.9936	0.9859	0.01522	0.02998
Double exponential degradation	0.08368	0.2001	0.9862	0.9811	0.9859	0.9808	0.02259	0.03493

From the comparison of fitting results, it can be seen that in the fitting results of the Gaussian degradation model, SSE and RMSE are close to 0, while R^2 and R^2_{adj} are close to 1, which indicates that the Gaussian degradation model has a strong ability to describe the non-linear degradation characteristics of batteries. Among them, due to the influence of the experimental environment or the nonlinear strength of capacity degradation, the superiority of fit of the B05 battery is slightly better than that of the B06 battery. From the comprehensive view of the fitting curve and fitting evaluation index, compared with the traditional double exponential degradation model, the Gaussian degradation model has a higher fitting accuracy for degradation data and a stronger ability to describe nonlinear degradation features.

3.2 RUL prediction result analysis

To verify the feasibility of the improved WCO-PF algorithm, considering the influence of the length of training data on state estimation, two different prediction starting points are set for each battery, and the results are compared with the traditional PF algorithm. The maximum error (ME), mean absolute error (MAE), and RMSE are used to evaluate the accuracy and robustness of the algorithm, as shown in Equation (10).

$$\begin{cases} \mathrm{MAE} = \dfrac{1}{\mathrm{N}}\displaystyle\sum_{i=1}^{\mathrm{N}}\left|Z_r^i - Z_p^i\right| \\ \mathrm{RMSE} = \sqrt{\dfrac{\sum_{i=1}^{\mathrm{N}}\left(Z_r^i - Z_p^i\right)^2}{\mathrm{N}}} \end{cases} \tag{10}$$

In Equation (10), Z_r is the real capacity of the cycle k, and Z_p is the predicted capacity of the cycle k, and N represents the number of cycles. Among them, MAE and RMSE are commonly used indicators to evaluate the effectiveness of algorithms or models.

3.2.1 Experimental verification at SP = 40 cycles

Firstly, the length of the training data is 40 cycles, and the training data with a short length can test the adjustment time of the algorithm for data optimization. The longer the adjustment time, the longer the time needed to reach the optimal state, and the larger the calculation amount. When the SP is 40 cycles, the comparison of RUL prediction results between the traditional PF algorithm and the improved WCO-PF algorithm is shown in Figure 6.

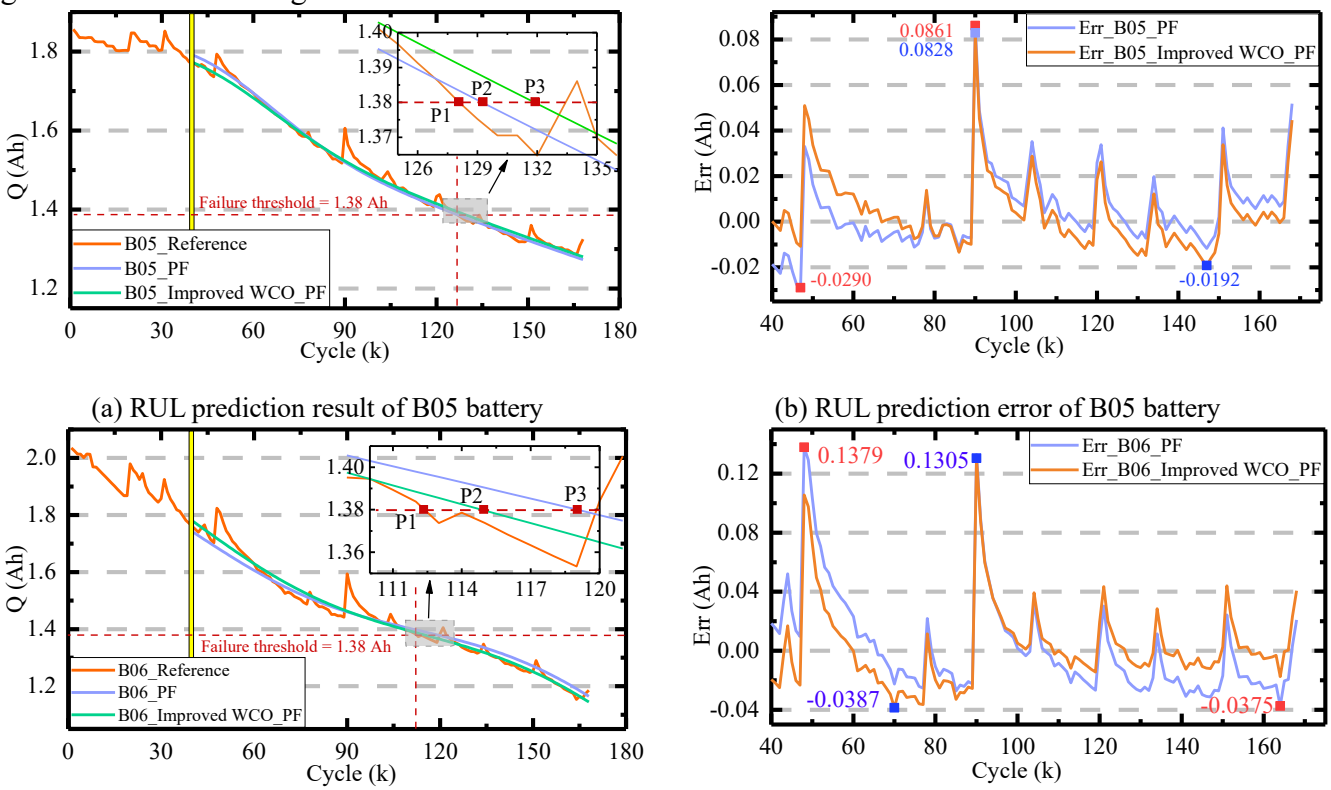

(a) RUL prediction result of B05 battery

(b) RUL prediction error of B05 battery

(c) RUL prediction result of B06 battery

(d) RUL prediction error of B06 battery

Figure 6. Comparison between predicted and actual RUL at the starting point of 40 cycles

Figure 6 (a) shows the prediction results of the B05 battery, where P1 represents the real failure point with a value of 128, P2 represents the predicted failure point for PF with a value of 130, and P3 represents the predicted failure point for improving WCO-PF with a value of 132. In the prediction of the B05 battery, the error between the traditional PF algorithm and real value is 2 cycles, while the error between improved WCO-PF and true value is 4 cycles, and it is larger than the traditional PF algorithm, which is an accidental phenomenon and the overall error needs to be further compared. Figure 6 (c) shows the prediction result for the B06 battery, where P1 represents the real failure point with a value of 113, P2 represents the predicted failure point to improve WCO-PF with a value of 115, P3 represents the predicted failure point of PF with a value of 119, which leads to an error of 2 cycles for the improved WCO-PF algorithm and 6 cycles for the traditional PF algorithm. In Figures 6 (b) and (d), the blue curve is the prediction error of the traditional

PF algorithm, and the orange curve is the prediction error of the improved WCO-PF algorithm. It can be seen that the error of the improved WCO-PF algorithm always fluctuates around 0 and is more stable than the traditional PF algorithm. The ME, MAE and RMSE can be observed and calculated by using Equation (10) as shown in Table 3.

Table 3. Comparison of RUL prediction results at 40 cycles

Estimation algorithm	PF		Improved WCO - PF	
	B05	B06	B05	B06
ME	8.61%	13.79%	8.28%	13.05%
MAE	0. 87%	1.87%	0. 82%	1.44%
RMSE	1. 45%	2.97%	1. 40%	2.45%

It can be seen from Table 3, for the ME of the capacity prediction error, the prediction results of the improved WCO-PF algorithm for the two groups of batteries are improved by 0.33% and 0.74% respectively compared with the traditional PF algorithm. For the MAE and RMSE of capacity prediction errors, it can be seen that the prediction errors of the improved WCO-PF algorithm are lower than the traditional PF algorithm, which proves that the improved algorithm has a better overall prediction effect and stronger tracking performance. According to the RUL prediction results of different algorithms on different batteries in Table 3, a visual diagram as shown in Figure 7 can be obtained.

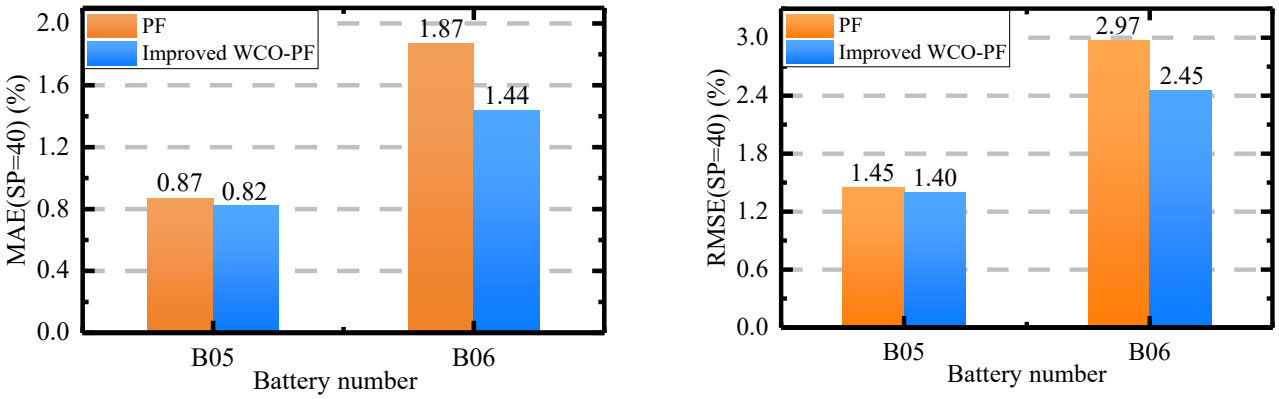

(a) Comparison of MAE at SP=40 (b) Comparison of MAE at SP=70

Figure 7. MAE and RMSE bar comparison graph of overall prediction results at SP = 40

It can be seen from Figure 7 (a), the MSE of the improved WCO-PF algorithm for the RUL estimation results of B05 and B06 batteries at SP=40 are 0.82% and 1.44% respectively, which are 0.05% and 0.43% higher compared to the traditional PF algorithm. From Figure 7 (b), the RMSE of the improved WCO-PF algorithm for the RUL estimation results of B05 and B06 batteries at SP=40 are 1.40% and 2.45% respectively, which are 0.05% and 0.52% higher compared to the traditional PF algorithm, which proves that the improved algorithm has better prediction ability.

3.2.2 Experimental verification at SP = 70 cycles

To further verify the improvement effect of the improved WCO-PF algorithm and the adaptability to different training data lengths, the amount of data used to update model parameters is increased with the SP setting to 70 cycles. The comparison of RUL prediction results between the traditional PF algorithm and the improved WCO-PF algorithm is shown in Figure 8.

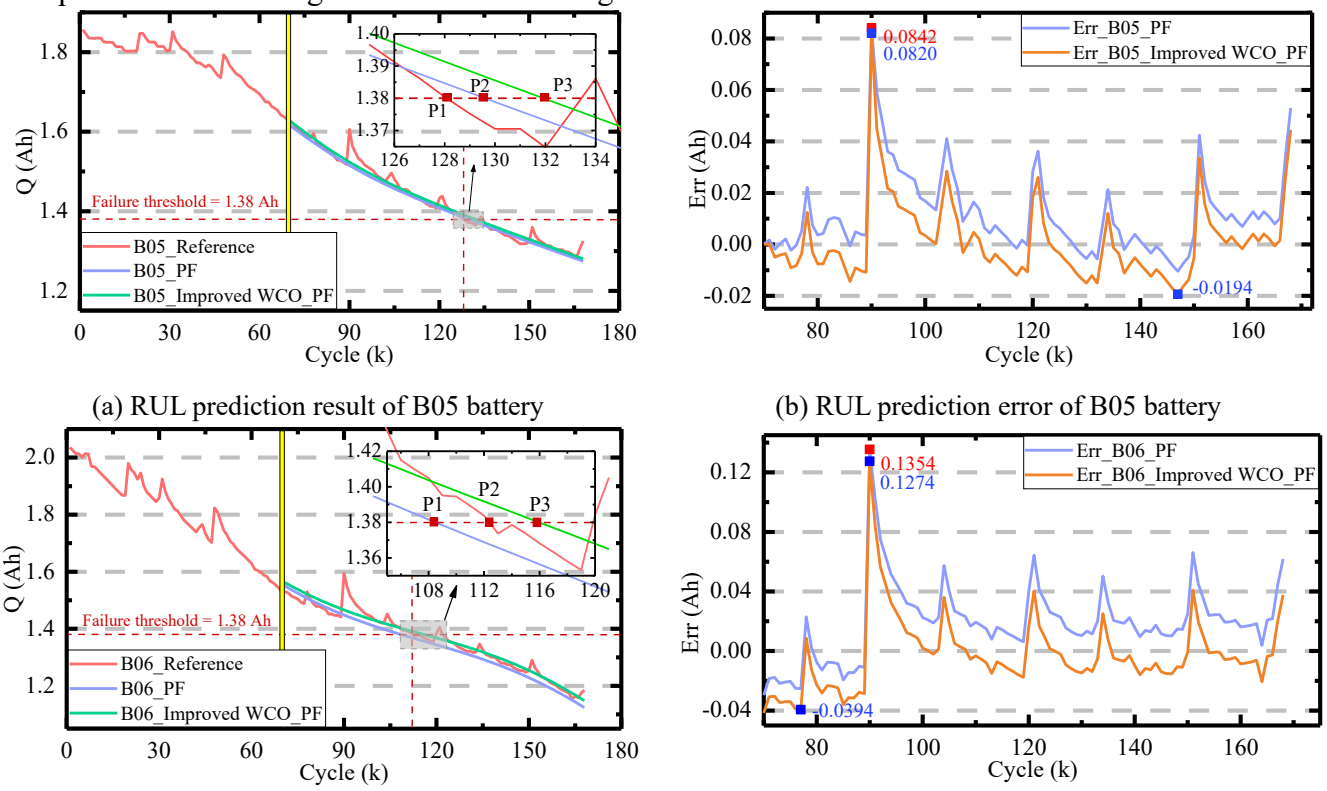

(a) RUL prediction result of B05 battery

(b) RUL prediction error of B05 battery

(c) RUL prediction result of B06 battery

(d) RUL prediction error of B06 battery

Figure 8. Comparison between predicted and actual RUL at the starting point of 70 cycles

Figure 8 (a) shows the prediction results of the B05 battery, where P1 is the real failure point with a value of 128, P2 is the predicted failure point for PF with a value of 129, and P3 is the predicted failure point for improving WCO-PF with a value of 132. In the prediction of the B05 battery, the error between the traditional PF algorithm and real value is 2 cycles, while the error between improved WCO-PF and real value is 4 cycles which is larger than the traditional PF algorithm, so the overall error needs to be further compared. Figure 8 (c) shows the prediction failure point of the B06 battery, where P1 is the predicted failure point of the improved WCO-PF with a value of 108, P2 is the actual failure point with a value of 113, P3 is the predicted failure point of PF with a value of 116, which leads to an error of 3 cycles for the improved WCO-PF algorithm and 5 cycles for the traditional PF algorithm. In Figure 8 (b) and (d), the blue curve is the prediction error of the traditional PF algorithm, and the orange curve is the prediction error of the improved WCO-PF algorithm which shows that the improved WCO-PF has a better prediction effect

than the traditional PF. The ME, MAE and RMSE can be observed and calculated by using Equation (10) as shown in Table 4.

Table 4. Comparison of RUL prediction results at 70 cycles

Estimation algorithm	PF		Improved WCO - PF	
	B05	B06	B05	B06
ME	8.42%	13.54%	8.20%	12.74%
MAE	0.67%	1.49%	0.61%	1.03%
RMSE	1.35%	2.50%	1.17%	1.93%

It can be seen from Table 4, for the ME of capacity prediction error, the prediction results of the improved WCO-PF algorithm for the two batteries are improved by 0.22% and 0.80% respectively to the traditional PF algorithm, which proves that the improved algorithm still has high accuracy. For the MAE and RMSE of capacity prediction errors, it can be seen that the prediction errors of the improved WCO-PF algorithm are lower than the traditional PF algorithm, which proves that the improved algorithm has strong comprehensive ability. According to the RUL prediction results of different algorithms on different batteries in Table 4, a visual diagram as shown in Figure 9 can be obtained.

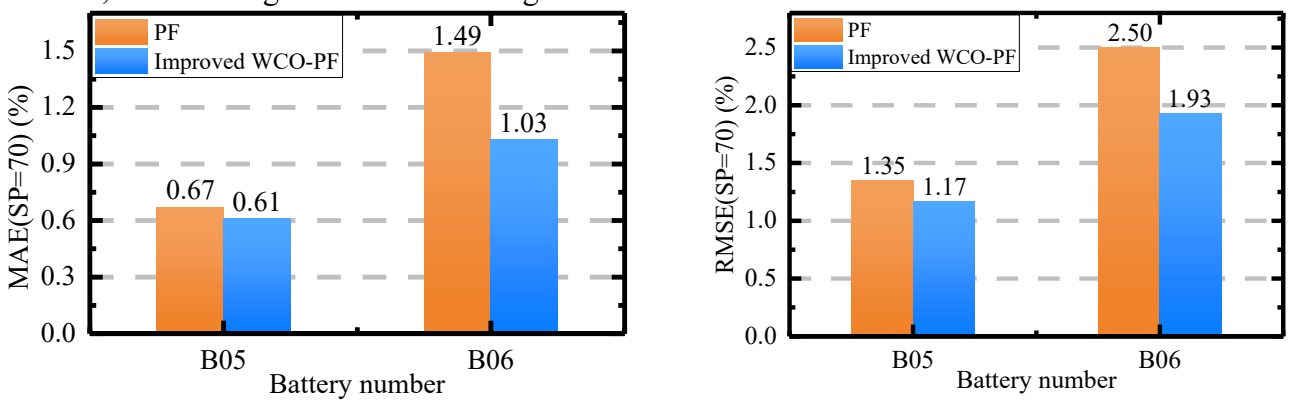

(a) Comparison of RMSE at SP=40 (b) Comparison of RMSE at SP=70

Figure 9. RMSE bar comparison graph of overall prediction results

It can be seen from Figure 9 (a), the MAE of the improved WCO-PF algorithm for the RUL estimation results of B05 and B06 batteries at SP=70 are 0.61% and 1.03% respectively, which are 0.06% and 0.46% higher compared to the traditional PF algorithm. In addition, by comparing the MAE of the improved WCO-PF algorithm at SP=40 in Figure 7 (a) and SP=70, it can be concluded that the MAE of B05 and B06 batteries are increased by 0.21% and 0.41% respectively. The RMSE of the improved WCO-PF algorithm for the RUL estimation results of B05 and B06 batteries at SP=70 are 1.17% and 1.93% respectively, which are 0.18% and 0.57% higher compared to the traditional PF algorithm. In addition, by comparing the RMSE of the improved WCO-PF algorithm at SP=40 in Figure 7 (b) and SP=70, it can be concluded that the

RMSE of B05 and B06 batteries are increased by 0.23% and 0.52% respectively, indicating that the improved algorithm has strong adaptability to different lengths of training data, and the increase of training data can indeed improve the accuracy of training results.

The above comparison shows that the improved WCO-PF algorithm has a strong optimization ability and tracking ability compared with the traditional PF, which can effectively improve the estimation accuracy of the RUL of lithium-ion batteries. Meanwhile, by analyzing the prediction results obtained from different SPs, it can be proved that the improved WCO-PF algorithm has strong adaptability to training data while ensuring prediction accuracy, and the increase of training data can improve the estimation accuracy of the algorithm.

4 Conclusions

Accurate estimation of remaining useful life is of great significance to ensure the safety and reliability of lithium-ion batteries in the whole life cycle. In this study, a new Gaussian degradation model is proposed, which greatly improves the fitting accuracy compared with the traditional double exponential degradation model. On the basis of the traditional particle filtering algorithm, an improved weighting coefficient optimization particle filtering method is proposed. Particles with relatively large weight coefficients are selected from a large number of candidate particles for state estimation to solve the problem of degradation and improve the diversity of sample sets, which largely solves the problem of "particle degradation" and "sample poverty" in traditional particle filtering. Among them, when using the training results to predict the value of future remaining useful life, the data matrix of the previous training results is processed as a whole to optimize the estimation effect. Finally, the battery aging data provided by the National Aeronautics and Space Administration is used for experimental verification. From the experimental results and analysis, it can be seen that the improved weighting coefficient optimization - particle filtering algorithm based on the Gaussian degradation model is effective and feasible for the remaining useful life estimation of lithium-ion batteries with high accuracy, which provides a solid theoretical basis for the accurate prediction of the remaining useful life, and is of great significance for the safety and reliability of lithium-ion batteries.

The algorithm and model proposed in this study still have a little shortage. The aging model cannot characterize the capacity recovery effect during the batteries degradation process and the improved weighting coefficient optimization algorithm has no standard for selecting particles with larger weights. Based on this study, considering the capacity recovery effect in the degradation process of lithium-ion batteries and considering the particle filtering process to make more particles converge to the optimal value to improve particle utilization will become the main content of future study.

ACKNOWLEDGMENTS

The work was supported by the National Natural Science Foundation of China (No. 62173281).

References

1. Hu, X.S., et al., *Battery Lifetime Prognostics.* Joule, 2020. **4**(2): p. 310-346.
2. Jiang, C., et al., *A state-of-charge estimation method of the power lithium-ion battery in complex conditions based on adaptive square root extended Kalman filter.* Energy, 2021. **219**: p. 1-11.
3. Wang, Y., et al., *A comprehensive review of battery modeling and state estimation approaches for advanced battery management systems.* Renewable and Sustainable Energy Reviews, 2020. **131**: p. 1-18.
4. Wang, X., et al., *Study on Remaining Useful Life Prediction of Lithium-ion Batteries Based on Charge Transfer Resistance.* Journal of Mechanical Engineering, 2021. **57**(14): p. 105-117.
5. Dai, H.F., et al., *Advanced battery management strategies for a sustainable energy future: Multilayer design concepts and research trends.* Renewable & Sustainable Energy Reviews, 2021. **138**: p. 1-25.
6. Lin, X.Y., et al., *State of charge estimation with the adaptive unscented Kalman filter based on an accurate equivalent circuit model.* Journal of Energy Storage, 2021. **41**: p. 1-9.
7. Hong, G.X., et al., *An iterative model of the generalized Cauchy process for predicting the remaining useful life of lithium-ion batteries.* Measurement, 2022. **187**: p. 1-8.
8. Shi, H.T., et al., *Improved multi-time scale lumped thermoelectric coupling modeling and parameter dispersion evaluation of lithium-ion batteries.* Applied Energy, 2022. **324**: p. 1-28.
9. Ye, M., et al., *Model-based state-of-charge estimation approach of the Lithium-ion battery using an improved adaptive particle filter.* Energy Procedia, 2016. **103**: p. 394-399.
10. Shen, D.X., et al., *A novel online method for predicting the remaining useful life of lithium-ion batteries considering random variable discharge current.* Energy, 2021. **218**: p. 1-17.
11. Jia, J.F., et al., *SOH and RUL Prediction of Lithium-Ion Batteries Based on Gaussian Process Regression with Indirect Health Indicators.* Energies, 2020. **13**(2): p. 1-20.
12. Wu, J., C.B. Zhang, and Z.H. Chen, *An online method for lithium-ion battery remaining useful life estimation using importance sampling and neural networks.* Applied Energy, 2016. **173**: p. 134-140.
13. Zhang, C.Y., et al., *Improved Particle Swarm Optimization-Extreme Learning Machine Modeling Strategies for the Accurate Lithium-ion Battery State of Health Estimation and High-adaptability Remaining Useful Life Prediction.* Journal of the Electrochemical Society, 2022. **169**(8): p. 1-10.
14. Ge, M.F., et al., *A review on state of health estimations and remaining useful life prognostics of lithium-ion batteries.* Measurement, 2021. **174**: p. 1-27.
15. Wang, S.L., et al., *A critical review of improved deep learning methods for the remaining useful life prediction of lithium-ion batteries.* Energy Reports, 2021. **7**: p. 5562-5574.
16. Pan, C.F., et al., *Prediction of remaining useful life for lithium-ion battery based on particle filter with residual resampling.* Energy Science & Engineering, 2021. **9**(8): p. 1115-1133.
17. Wang, F.K., et al., *Online remaining useful life prediction of lithium-ion batteries using bidirectional long short-term memory with attention mechanism.* Energy, 2022. **254**: p. 1-10.
18. Cadini, F., et al., *State-of-life prognosis and diagnosis of lithium-ion batteries by data-driven particle filters.* Applied Energy, 2019. **235**: p. 661-672.
19. Hu, W.Y. and S.S. Zhao, *Remaining useful life prediction of lithium-ion batteries based on wavelet denoising and transformer neural network.* Frontiers in Energy Research, 2022. **10**: p. 1-13.
20. Wu, T.Z., T. Zhao, and S.Y. Xu, *Prediction of Remaining Useful Life of the Lithium-Ion Battery Based on Improved*

Particle Filtering. Frontiers in Energy Research, 2022. **10**: p. 1-11.

21. He, N., C. Qian, and L.L. He, *Short-Term Prediction of Remaining Life for Lithium-Ion Battery Based on Adaptive Hybrid Model With Long Short-Term Memory Neural Network and Optimized Particle Filter.* Journal of Electrochemical Energy Conversion and Storage, 2022. **19**(3): p. 1-13.
22. Liu, W.J., Y. Shen, and L.J. Shen, *Degradation Modeling for Lithium-Ion Batteries with an Exponential Jump-Diffusion Model.* Mathematics, 2022. **10**(16): p. 1-18.
23. Zhao, G., Y. Wang, and Z. Chen, *Health-aware multi-stage charging strategy for lithium-ion batteries based on whale optimization algorithm.* Journal of Energy Storage, 2022. **55**: p. 1-9.
24. Li, K., Y. Wang, and Z. Chen, *A comparative study of battery state-of-health estimation based on empirical mode decomposition and neural network.* Journal of Energy Storage, 2022. **54**: p. 1-12.
25. Miao, Q., et al., *Remaining useful life prediction of lithium-ion battery with unscented particle filter technique.* Microelectronics Reliability, 2013. **53**(6): p. 805-810.
26. Xie, G., et al., *Remaining useful life prediction of lithium-ion battery based on an improved particle filter algorithm.* Canadian Journal of Chemical Engineering, 2020. **98**(6): p. 1365-1376.
27. Duan, B., et al., *Remaining useful life prediction of lithium-ion battery based on extended Kalman particle filter.* International Journal of Energy Research, 2020. **44**(3): p. 1724-1734.
28. Thelen, A., et al., *Augmented model-based framework for battery remaining useful life prediction.* Applied Energy, 2022. **324**: p. 1-18.
29. Wang, S.L., et al., *A Critical Review of Improved Deep Convolutional Neural Network for Multi-Timescale State Prediction of Lithium-Ion Batteries.* Energies, 2022. **15**(14): p. 1-27.
30. Yang, X., et al., *Fuzzy adaptive singular value decomposition cubature Kalman filtering algorithm for lithium-ion battery state-of-charge estimation.* International Journal of Circuit Theory and Applications, 2022. **50**(6): p. 2287-2287.
31. Du, X.W., et al., *Remaining useful life prediction of Lithium-ion batteries of stratospheric airship by model-based method.* Microelectronics Reliability, 2019. **100**: p. 1-5.
32. Fan, Y.C., et al., *Incremental Capacity Curve Health-Indicator Extraction Based on Gaussian Filter and Improved Relevance Vector Machine for Lithium-Ion Battery Remaining Useful Life Estimation.* Metals, 2022. **12**(8): p. 1-17.
33. Qiu, J.S., et al., *Research on the remaining useful life prediction method of lithium-ion batteries based on aging feature extraction and multi-kernel relevance vector machine optimization model.* International Journal of Energy Research, 2022. **46**(10): p. 13931-13946.
34. Chen, L., et al., *Remaining useful life prediction for lithium-ion battery by combining an improved particle filter with sliding-window gray model.* Energy Reports, 2020. **6**: p. 2086-2093.
35. Xue, Z.W., et al., *Remaining useful life prediction of lithium-ion batteries with adaptive unscented kalman filter and optimized support vector regression.* Neurocomputing, 2020. **376**: p. 95-102.
36. Zhang, Y., et al., *Weight optimized unscented Kalman filter for degradation trend prediction of lithium-ion battery with error compensation strategy.* Energy, 2022. **251**: p. 1-12.
37. Guha, A., K.V. Vaisakh, and A. Patra, *Remaining useful life estimation of lithium-ion batteries based on a new capacity degradation model.* 2016 IEEE Transportation Electrification Conference and Expo, Asia-Pacific (ITEC Asia-Pacific), 2016: p. 1-6.